followed by EBER-ISH as described above. By using a Dako DuoCISH™, which is a double staining chromogenic in situ hybridization kit, EBV-infected B- or T-cells became visible by their blue nuclei and red membrane staining.

Results

Pathologic findings

LN1

The lymph node architecture was destroyed by diffuse proliferation of small to large lymphoid cells accompanied by numerous clusters of epithelioid histiocytes, giving a lymphoepithelioid appearance (Lennert lymphoma) (Fig. 1). Vascular proliferation was found but not prominent. Proliferating lymphoid cells had a round to oval shaped nucleus with slight nuclear indentation, in which one to several small nucleoli were discernible. Cytoplasm was clear and moderate to voluminous in amount. We noted bizarre cells showing mononuclei with occasional, relatively distinct nucleoli, but cells resembling Sternberg–Reed cells were absent. Mitotic figures were occasional. Plasma cells were few in number, and eosinophils were scarce. Immunohistochemistry revealed that the small to large lymphoid cells were CD20−, CD79a−, CD3+, CD4+, and CD8−. A diagnosis of PTCL of a lymphoepithelioid variant ("Lennert lymphoma") was made. Large lymphoid cells with CD20+ and/or CD79a+ were few in number.

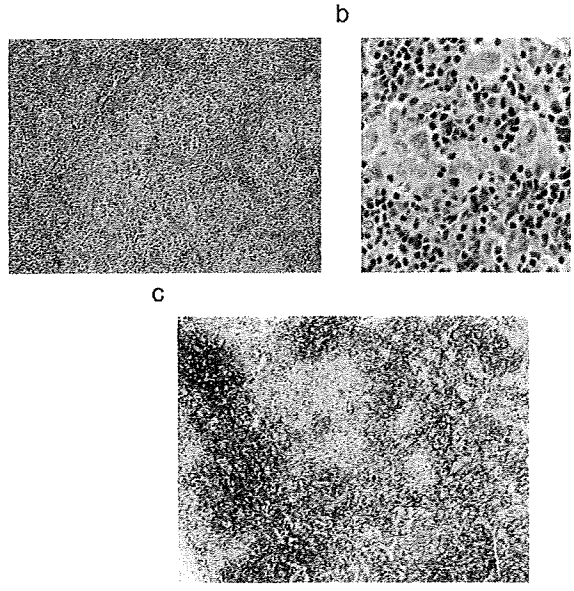

Fig. 1. LN1: (a) lymph node architecture was destroyed by diffuse proliferation of small to large lymphoid cells accompanied by numerous clusters of epithelioid histiocytes, giving a lymphoepithelioid appearance. H&E, × 100. (b) The majority of lymphoid cells were small to medium in size, with occasional large lymphoid cells. H&E, × 400. (c) Lymphoid cells were CD3+. ABC method, × 40.

LN2

Both the cervical and inguinal lymph nodes showed a histologic picture similar to that of LN1. However, immunohistochemically, the pattern of the large lymphoid cells was quite different from that of the initial biopsy (LN1), i.e., the majority were CD20+, CD79a+, CD3−, CD4−, CD8− and a few cells were CD3+, CD4+, CD8− (Fig. 2a–d). Large lymphoid cells with CD20+ and/or CD79a+ immunophenotypes had a round to oval nucleus in which one to several nucleoli adhering to nuclear membrane were discernible. Cytoplasm was scanty in these cells. Mitotic figures were occasional. These large lymphoid cells were CD10− and bcl6−. Vascular proliferation persisted but was not prominent.

Skin lesions (S1 and S2)

S1 and S2 showed the similar histologic picture, but denser lymphoid cell infiltration was found in S2. There was diffuse proliferation of small to large lymphoid cells with morphologic features similar to those found in LN1 in the upper dermis with obvious epidermotropism. Clusters of epithelioid histiocytes were not found in the skin lesion. Immunohistochemistry revealed that the small to large lymphoid cells were CD20−, CD3+, CD4+, CD8−, and those showing CD20+, CD3−, CD4−, CD8− were not found.

Clonality analysis

Gene rearrangement study on the LN1 lesion revealed the monoclonal bands for T-cell receptor (TCR)-β and TCR-γ chain genes, while only smears were found for immunoglobulin heavy (IgH) and light chain (IgL) genes. In the LN2 lesions, monoclonal bands were detected for TCR-β, TCR-γ, and TCR-δ chains, with electrophoretic patterns of bands and sizes identical to those found in the LN1 lesion. Furthermore, monoclonal bands for IgL were found in the LN2 lesions. These findings indicate a continuous proliferation of the same clone of T lymphocytes through the course and evolution of B-cell clone. In S2, monoclonal bands having the same sizes of those found in LN1 and LN2 were detected for TCR-γ chain, but monoclonal bands for IgH and IgL could not be detected (Fig. 3). S1 was insufficient for clonality analysis because of severe fragmentation of DNA.

Please cite this article as: T. Chihara, et al., Peripheral T-cell lymphoma of Lennert type complicated by monoclonal proliferation of large B-cells, Pathol. Res. Practice (2009), doi:10.1016/j.prp.2009.04.009

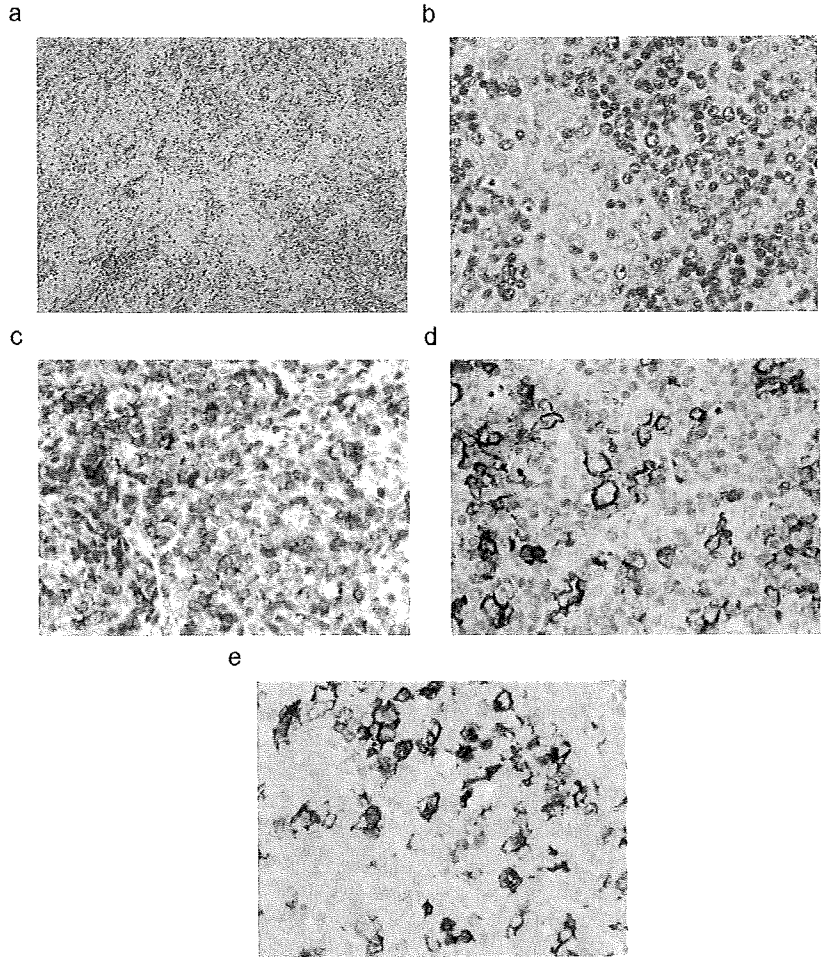

Fig. 2. LN2: (a) histologic picture similar to that of Fig. 1(a). H&E, × 100. (b) The majority of large lymphoid cells have round nuclei. Several nucleoli are adhered to nuclear membrane, resembling centroblasts. H&E, × 400. (c) The majority of CD3+ lymphoid cells were CD4+. ABC method, × 400. (d) There were many CD20+ large lymphoid cells. ABC method, × 400. (e): Double staining with CD20 and EBER-ISH. CD20+ large lymphoid cells contained Epstein-Barr virus genome in their nucleus. × 400.

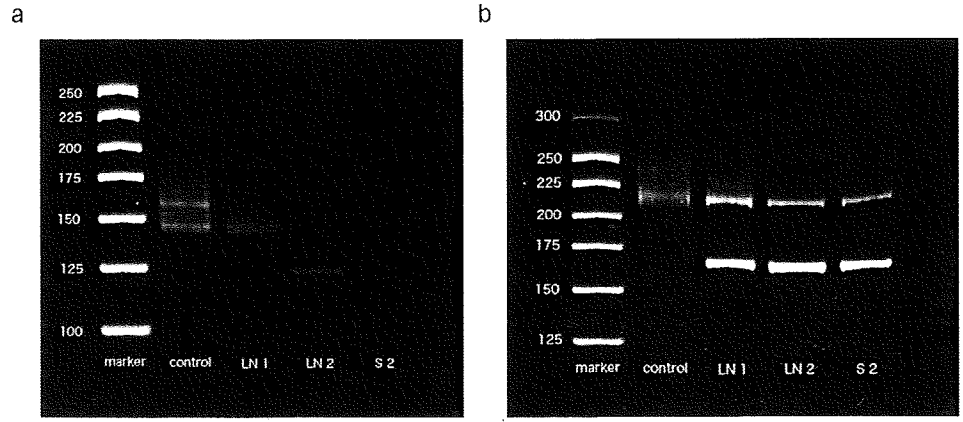

Fig. 3. Clonality analysis of LN1, LN2 and S2: (a) BIOMED-2 IGL. Monoclonal bands were found in the LN2, but germline smear configuration in LN1 and S2. (b) BIOMED-2 TCR-G-A. Monoclonal and same size bands were found in LN1, LN2, and S2.

Please cite this article as: T. Chihara, et al., Peripheral T-cell lymphoma of Lennert type complicated by monoclonal proliferation of large B-cells, Pathol. Res. Practice (2009), doi:10.1016/j.prp.2009.04.009

In situ hybridization for EBV

In situ hybridization revealed positive signals in the nucleus of large lymphoid cells in LN2 but not in LN1, S1, and S2. Double staining with immunohistochemistry using anti-CD20 and CD3 antibodies and in situ hybridization with EBER-1 probe on the LN2 revealed that only the CD20-positive large lymphoid cells contained EBV genome in their nucleus (Fig. 2e).

Discussion

The present case shows the histologic and immunohistochemical features that are typical of the "Lennert lymphoma" in the initial biopsy taken from the inguinal lymph node (LN1), i.e., diffuse proliferation of small to large lymphoid cells of CD3+, CD4+, and CD8− immunophenotype accompanied by numerous clusters of epithelioid histiocytes. In the subsequent biopsy taken from the cervical and inguinal lymph nodes 5 years after the onset of disease (LN2), the large cells with CD3+, CD4+, and CD8− decreased in number, although clonality analysis revealed the persistence of an identical T-cell clone found in LN1, confirming the recurrence of the "Lennert lymphoma". While proliferation of B-cells was not evident histologically and immunohistochemically, and clonal proliferation was not detectable by clonality analysis for LN1, there were numerous large B lymphoid cells in LN2. Molecular analysis confirmed the presence of B-cell clone, indicating the evolution of DLBCL. The "Lennert lymphoma" recurred on the skin, with no evidence of concomitant B-cell clone. Taken together, it could be concluded that the DLBCL evolved transiently during the course of "Lennert lymphoma".

Reports on the evolution of secondary B-cell lymphoma during the course of PTCL have accumulated recently (Table 1). AILT is the representative of PTCL for the development of secondary B-cell lymphoma [2,5] although much less frequently, other kinds of PTCL could be a basis for the development of B-cell lymphoma [4,5,10]. The clonality of T- and B-cells in

Table 1. Summary of reported cases on the evolution of B-cell lymphoma in the course of peripheral T-cell lymphoma.

Case	Initial lymphoma				Secondary lymphoma				Interval between two lymphomas (months)	
	Disease	EBV	TC	BC	Disease	EBV	TC	BC		
1	AILT	na	na	na	DLBCL	+	P	M	34	
2	AILT	na	M	P	DLBCl	+	P	O	29	
3	PTCL, NOS	na	M	P	DLBCL	+	P	P	40	
4	AILT	na	**B***	P	Plasmacytoma	+	**M***	O	96	
5	PTCL	+	M	O	DLBCL	–	P	M	12	
6	PTCL	+	M	M	DLBCL	na	na	na	22	
7	AILT	na	na	na	DLBCL	na	P	P	21	
8	AILT	na	na	na	DLBCL	na	na	M	12	
9	AILT	na	na	na	DLBCL	na	P	M	3	
10	AILT	na	na	na	DLBCL	+	na	na	8	
11	AILT	na	na	na	DLBCL	na	na	na	15	
12	AILT	na	na	na	DLBCL	+	M	M	5	
13	AILT	na	na	na	cHL	+	M	P	21	
14	AILT	na	na	na	cHL	+	M	P	31	
15	AILT	na	na	na	DLBCL	+	na	na	24	
16	AILT	+	**M***	P	AILT+DLBCL	+	**M***	M	8	
17	AILT	+	M	P	cHL	+	P	P	63	
18	AILT	+	M	na	cHL	+	P	P	60	
19	AILT	na	na	na	DLBCL	+	M	M	8	
20	AILT	na	M	M	DLBCL	+	P	M	84	
21	AILT	na	na	na	DLBCL	–	na	na	8	
22	PTCL, NOS	na	na	na	PTCL+DLBCL	na	na	na	14	
									Mean	28.1
23	PTCL-U	–	**M***	P	PTCL+DLBCL	+	**M***	M	58	

TC: T-cell clone; BC: B-cell clone; EBV: Epstein-Barr virus; na: data not available; M: monoclonal; P: polyclonal; B: biclonal; O: oligoclonal; +: present; –: absent; AILT: angioimmunoblastic T-cell lymphoma; cHL: classical Hodgkin lymphoma; PTCL, NOS: peripheral T-cell lymphoma, not other specified.
Refs. for cases 1–4 [10]; 5 and 6 [4]; 7–14 [9]; 15–21 [2]; 22 [5]; 23, present case.
The bold character **M** denotes presence of monoclonality.

Please cite this article as: T. Chihara, et al., Peripheral T-cell lymphoma of Lennert type complicated by monoclonal proliferation of large B-cells, Pathol. Res. Practice (2009), doi:10.1016/j.prp.2009.04.009

initial and second biopsies was examined in 7 of 22 previously reported cases (Cases 2, 3, 4, 5, 16, 17, 20) (Table 1): only two cases showed the presence of the same T-cell clone in the serial biopsy (Cases 4 and 16). In the second biopsy, oligoclonal or monoclonal B-cells were revealed in 10 cases, among which oligoclonal or monoclonal B-cell proliferation was present even in the initial biopsy of three cases (Cases 5, 6, and 20). The evolution of clonal B-cells in the second biopsy was shown in three cases (Cases 2, 4, and 16). The simultaneous occurrence of PTCL and DLBCL in the second biopsy was confirmed at the morphological level in two cases (Cases 16 and 22) and at the molecular level in four (Cases 4, 12, 16, and 19). The diagnosis of composite PTCL and DLBCL was justified because both lesions were confirmed at both the morphologic and molecular level in one of the reported cases (Case 16). This report is the first to show the evolution of B-cell lymphoma during the course of "Lennert lymphoma", justified not only by morphology but also on a molecular basis. The interval between the onset of PTCL and the development of secondary B-cell lymphoma ranged from 3 to 96 (mean 28.1) months in the previous reports [2,4,5,9,10], and was 58 months in the present case.

An immunodeficient condition induced in individuals with AILT is supposed to provide a basis for the development of B-cell lymphoma [10,2,9]. It is well-known that EBV genome is frequently detected in lymphoma cells, mostly in B-cell lymphomas, in immunocompromised hosts such as acquired immunodeficiency syndrome and organ transplant recipients, receiving immunodepressants [1,3,6]. In the previous reports on PTCL, concomitant or evolving B-cell lymphomas were usually EBV-positive [2,5,7]. In situ hybridization together with immunohistochemical procedures employed in the present case clearly showed that the EBV genome was present exclusively in the nucleus of large B-lymphoid cells in the evolving DLBCL. These findings suggest the appearance of an immunodeficient condition in the course of the "Lennert lymphoma", which provides the basis for the development of EBV-positive DLBCL.

In the present case, it is difficult or even impossible to diagnose composite Lennert lymphoma and DLBCL on morphologic grounds alone. For this, a combination of immunohistochemical and clonality analysis is indispensable. Regarding the point of treatment, it is important to be aware of the behavior of evolving DLBCL in cases with PTCL. Information for this is quite limited at present. Is it necessary to change the therapeutic modality? What is the clinical relevance of recognizing this kind of phenomenon? How about the prognosis of patients affected by the secondary B-cell lymphoma? An accumulation of well-characterized cases is necessary to answer these questions.

In this case, the EBV-positive large B-cell lymphoma appeared transiently in the course of the "Lennert lymphoma". Clonality analysis was indispensible to disclose the complex condition of this case.

Acknowledgments

The authors thank Ms. K. Fujikawa for her technical assistance and Mr. Y. Hatanaka, Dakocytomation, Kyoto, Japan, for his advice on the double staining.

References

[1] P. Andreone, A. Gramenzi, S. Lorenzini, et al., Post-transplantation lymphoproliferative disorders, Arch. Intern. Med. 163 (2003) 1997–2004.
[2] A.D. Atyygalle, C. Kyriakou, J. Dupuis, et al., Histologic evolution of angioimmunoblastic T-cell lymphoma in consecutive biopsies: clinical correlation and insights into natural history and disease progression, Am. J. Surg. Pathol. 31 (2007) 1077–1088.
[3] A. Carbone, A. Gloghini, G. Dotti, et al., EBV-associated lymphoproliferative disorders: classification and treatment, Oncologist 13 (2008) 577–585.
[4] J.P.T. Higgins, M. Van de Rijn, P.D. Carol, et al., Peripheral T-cell lymphoma complicated by a proliferation of large B Cells, Am. J. Clin. Pathol. 114 (2000) 236–247.
[5] W. Jun, W. Zhuo-Cai, C. Xiao-Dong, A case report of composite lymphoma, Chin. J. Cancer 26 (2007) 337–338.
[6] H. Tran, J. Nourse, S. Hall, et al., Immunodeficiency-associated lymphomas, Blood Rev. 22 (2008) 261–281.
[7] J.J.M. Van Dongen, A.W. Langerak, M. Bruggemann, et al., Design and standardization of PCR primers and protocols for detection of clonal immunoglobulin and T-cell receptor gene recombinations in suspect lymphoproliferations: Report of the BIOMED-2 Concerted Action BMH4-CT98-3936, Leukemia 17 (2003) 2257–2317.
[8] L.M. Weiss, E.S. Jaffe, X.F. Liu, Y.Y. Chen, D. Shibata, L.J. Medeiros, Detection and localization of Epstein-Barr viral genomes in angioimmunoblastic lymphadenopathy and angioimmunoblastic lymphadenopathy-like lymphoma, Blood 79 (1992) 1789–1795.
[9] K. Willenbrock, A. Brauninger, M.-L. Hansmann, Frequent occurrence of B-cell lymphomas in angioimmunoblastic T-cell lymphoma and proliferation of Epstein-Barr virus-infected cells in early cases, Br. J. Haematol. 138 (2007) 733–739.
[10] A. Zettl, S.-S. Lee, T. Rudiger, et al., Epstein-Barr virus-associated B-cell lymphoproliferative disorders in angioimmunoblastic T-cell lymphoma and peripheral T-cell lymphoma, unspecified, Am. J. Clin. Pathol. 117 (2002) 368–379.

Please cite this article as: T. Chihara, et al., Peripheral T-cell lymphoma of Lennert type complicated by monoclonal proliferation of large B-cells, Pathol. Res. Practice (2009), doi:10.1016/j.prp.2009.04.009

Int J Clin Oncol (2009) 14:150–158
DOI 10.1007/s10147-008-0823-x

ORIGINAL ARTICLE

Mitsuaki Tatsumi · Hiroyuki Sugahara · Ichiro Higuchi
Hiroki Fukunaga · Hironobu Nakamura
Yuzuru Kanakura · Jun Hatazawa

Standardized uptake value on FDG-PET as a marker for disease activity in patients with non-Hodgkin's lymphoma: comparison with serum soluble interleukin-2 receptor values

Received: March 27, 2008 / Accepted: July 14, 2008

Abstract
Background. We compared standardized uptake values (SUVs) on positron emission tomography with a glucose analog, 2-[F-18] fluoro-2-deoxy-D-glucose (FDG-PET) and serum soluble interleukin-2 receptor (sIL-2R) values in patients with non-Hodgkin's lymphoma (NHL) in the pre-, mid- (after three or four cycles), and post-treatment periods of chemotherapy (pre, mid, and post, respectively), and we examined whether the SUV was a useful tumor marker for NHL.
Methods. The SUVs on PET and sIL-2R values were retrospectively evaluated based on all the clinical information available in 40 patients (31 in pre, 24 in mid, and 24 in the post periods). Patients in complete remission status were classified as group A and those with active residual disease in the mid and post periods were classified as group B.
Results. In pre, the SUV and sIL-2R values exhibited sensitivity of 100% and 84%, respectively. In mid, the SUV was lower in group A than in group B, while sIL-2R was not different. The SUV yielded better specificity than sIL-2R (88 % vs 25 %, respectively), though the difference was not significant. In mid, the SUV in patients later assigned to group A in post was lower than than the SUV in group B, whereas sIL-2R was not different. In post, the specificity and accuracy of SUV were better than those of sIL-2R (95 vs 47 %, and 96 vs 58 %, respectively). Both the SUV and sIL-2R were lower in group A than in group B.
Conclusion. The SUV on PET was better than the serum sIL-2R as a marker to evaluate the disease status of NHL, and was considered to be a useful tumor marker for NHL.

Key words Standardized uptake value · FDG-PET · Non-Hodgkin's lymphoma · Serum soluble interleukin-2 receptor

M. Tatsumi (✉) I. Higuchi J. Hatazawa
Department of Nuclear Medicine, Osaka University Graduate School of Medicine, 2-2-D9 Yamadaoka, Suita, Osaka 565-0871, Japan
Tel. +81-6-6879-3461; Fax +81-6-6879-3469
e-mail: m-tatsumi@radiol.med.osaka-u.ac.jp

M. Tatsumi H. Nakamura
Department of Radiology, Osaka University Graduate School of Medicine, Suita, Osaka, Japan

H. Sugahara Y. Kanakura
Department of Hematology and Oncology, Osaka University Graduate School of Medicine, Suita, Osaka, Japan

I. Higuchi · H. Fukunaga
Department of Surgery and Clinical Oncology, Osaka University Graduate School of Medicine, Suita, Osaka, Japan

Introduction

Non-Hodgkin's lymphoma (NHL) is one of the malignancies that are basically treated nonsurgically, and effective therapeutic regimens, including multidrug chemotherapy and/or radiotherapy, have been established for this disease. In addition to these established regimens, new treatment options, such as high-dose chemotherapy with bone marrow or stem cell transplantation,[1–3] or radioimmunotherapy,[4] have been developed and applied to the treatment of high-risk or relapsed lymphoma in recent years. Accurate monitoring of disease status and early detection of relapse are critical, because the new treatment options should be performed early in patients who are not expected to experience a longstanding complete remission (CR) based on conventional therapeutic regimens.

The serum soluble interleukin-2 receptor (sIL-2R), a truncated form of the receptor secreted by activated T cells, has recently been used clinically as a marker of tumor burden and disease activity in NHL, as well as in other hematological malignancies.[5–14] The lowest serum sIL-2R values are usually observed in patients with a single tumor mass or in those with CR status after treatment, whereas the highest values are frequently observed in patients with multiple tumors and more extensive systemic disease. The sIL-2R values are considered to be a better marker for NHL than the standard predictors of tumor burden, including serum lactic dehydrogenase (LDH) and uric acid levels.[11–14]

Positron emission tomography with a glucose analog, 2-[F-18] fluoro-2-deoxy-D-glucose (FDG-PET), has been used as a new imaging method in the field of oncology.[15-17] FDG-PET enables detection of the increased glucose uptake characteristic of malignant cells, and thus has been recognized as a valuable tool not only for initial diagnosis and staging but also for the detection of recurrences and evaluation of the chemo-/chemoradiotherapeutic response in various kinds of malignant tumors. FDG-PET, with its whole-body imaging technique, has been shown to be extremely useful in the staging and evaluation of treatment response in NHL.[18-21] On FDG-PET, the standardized uptake value (SUV) is frequently used to evaluate lesions semiquantitatively, along with the use of qualitative visual assessment.[22,23] However, no reports have been published to date on the relationship between SUVs and serum sIL-2R values, which are also frequently used as a hematological marker in the course of NHL treatment in Japan.

In the present study, we compared the SUVs on FDG-PET and serum sIL-2R values in patients with NHL in the pre-, mid- (after three or four cycles), and post-treatment periods of chemotherapy, and examined whether the SUV was a useful tumor marker for NHL.

Patients and methods

Patients

Forty patients (18 men and 22 women; mean age, 57 years) with biopsy-proven NHL who had had whole-body FDG-PET studies were retrospectively evaluated in this study. Although 5 patients with recurrence were included, a CR had been obtained by previous treatment without any evidence of residual mass or soft tissue in these patients. Nine patients (patients 21–24, 36–40; as numbered in Table 1) who did not undergo pretreatment FDG-PET studies were also included in this study, because the residual masses seen by morphological imaging were evaluated by PET during and/or after treatment in these patients. Based on the recent WHO classification,[24,25] 16 patients were classified as having indolent lymphomas and 24 were classified as having aggressive lymphomas. Patient characteristics are listed in Table 1.

All patients received chemotherapy, and 30 of them had the CHOP regimen (a combination of cyclophosphamide, doxorubicin, vincristine, and prednisone). Three patients were given radiation therapy before post-treatment PET evaluation. As diffuse and intense FDG uptake in the bone marrow caused by granulocyte colony-stimulating factor (G-CSF) administration could be a potential source of false-positive findings, we asked referring oncologists not to order PET examinations in patients when their bone marrow status was considered to be highly activated according to laboratory data.

Written informed consent was obtained from all patients, and the study was approved by the Ethics Committee of Osaka University Graduate School of Medicine. This study was performed in accordance with the ethical standards based on the 1995 Declaration of Helsinki.

Clinical examination

All patients were evaluated routinely by physical examination; laboratory studies including measurement of sIL-2R, LDH, and C-reactive protein (CRP) values; morphological imaging studies including contrast-enhanced computed tomography (CT) and/or magnetic resonance imaging (MRI) of the neck, chest, and abdomen/pelvis; and bone marrow biopsy within 14 days before the start of chemotherapy. Reevaluation was performed after three or four cycles of chemotherapy (midtreatment) and after completion of treatment (post-treatment). The area to be examined by morphological imaging and the requirement for bone marrow biopsy in the mid- and post-treatment periods were determined by oncologists according to the pretreatment disease status of each patient.

The serum sIL-2R values were measured by a sandwich enzyme immunoassay, in the form of an IMMULIZE Interleukin-2 Receptor Test Kit (EURO/DPC, Gwynedd, UK, supplied by DIA-IATRON, Tokyo, Japan), according to the manufacturer's instructions. This immunoassay uses two monoclonal antibodies that recognize different epitopes of the IL-2R α chain. The normal serum sIL-2R values range from 220 to 530 U/ml.

FDG-PET imaging

A total of 79 FDG-PET examinations for the 40 patients were evaluated in this study. Pretreatment PET examinations were performed within 10 days before the start of chemotherapy in 31 patients, midtreatment PET studies were performed approximately 10 days after finishing three or four cycles of chemotherapy in 24 patients, and post-treatment PET examinations were performed more than 10 days after completion of all treatments in 24 patients. Five patients (patients 1–5) underwent pre-, mid-, and post-treatment PET studies. 15 patients (patients 6–20) underwent pre- and midtreatment studies, 11 patients (patients 25–35) underwent pre- and post-treatment studies, and 3 patients (patients 22–24) underwent mid- and post-treatment studies. One patient (patient 21) had only midtreatment studies and 5 patients (patients 36–40) had only post-treatment studies.

Whole-body FDG-PET images were acquired with a Headtome V/SET 2400W (Shimadzu, Kyoto, Japan), which is capable of the simultaneous acquisition of 63 contiguous 3.1-mm-thick sections (20-cm total thickness) in one bed position. The intrinsic resolution at the center is 3.7 mm-FWHM, and the sensitivity of the device is 7300 cps/KBq. All patients fasted for at least 4 h before the examination. Simultaneous static emission-transmission scans (i.e., attenuation-corrected images) from the neck to symphysis were obtained 1 h after the injection of 370 MBq (10 mCi) of FDG, and if warranted by clinical suspicion, scans were

Table 1. Summary of clinical and PET data in each treatment period

Patient no	Age (years)/ Sex	Clinical group	Pretreatment				Midtreatment				Post-treatment			
			Clinical evaluation		PET evaluation		Clinical evaluation		PET evaluation		Clinical evaluation		PET evaluation	
			Stage	sIL-2R (U/ml)	Stage	SUV	Response/ Group	sIL-2R/% sIL-2R	Residual uptake	SUV/% SUV	Response/ Group	sIL-2R/% sIL-2R	Residual uptake	SUV/% SUV
1	48/ F	ID	II	694	II	6.1	PR/ B	598/ 86 2	M	2 2/ 35.7	CR/ A	478/ 68 9	N	1 2/ 19.5
2	49/ F	ID	III	1330	III	11 0	PR/ B	796/ 59 9	S	1 9/ 17.0	CR/ A	836/ 62.9	N	1.2/ 11 1
3	52/ F	ID	IV	3820	IV	5.7	PR/ B	645/ 16.9	S	1 8/ 31 1	CR/ A	764/ 20 0	N	1 4/ 25 1
4	72/ F	ID	IV	934	III	16 6	PR/ B	662/ 70 9	S	2.3/ 13 9	CR/ A	516/ 55 2	N	1 3/ 7.8
5	75/ M	AG	II	1990	II	11.1	PR/ B	980/ 49 3	S	2 8/ 24 8	CR/ A	712/ 35 8	N	1 9/ 17 3
6	54/ M	ID	I	457	I	3 8	PR/ B	436/ 95 4	S	2.8/ 73 5	NA	NA	NA	NA
7	47/ M	ID	II	1550	II	5 5	CR/ A	573/ 37 0	N	1 5/ 27 1	NA	NA	NA	NA
8	73/ F	ID	II	530	II	5.3	CR/ A	500/ 94 3	N	2 0/ 37.6	NA	NA	NA	NA
9	52/ F	ID	IV	2140	IV	2 9	CR/ A	1830/ 85 5	N	0 84/ 29.4	NA	NA	NA	NA
10	56/ F	ID	IV	1300	III	7 7	PR/ B	862/ 66.3	M	3 9/ 50 7	NA	NA	NA	NA
11	58/ M	ID	IV	15500	IV	6 7	CR/ A	1210/ 7.8	N	1 9/ 28 0	NA	NA	NA	NA
12	51/ F	AG	I	971	I	21.1	PR/ B	816/ 84 0	S	3.5/ 16.4	NA	NA	NA	NA
13	51/ F	AG	I	1120	I	16 0	PR/ B	910/ 81.3	S	1 5/ 9 5	NA	NA	NA	NA
14	58/ M	AG	I	159	I	18 5	CR/ A	105/ 66 0	N	2 8/ 15.0	NA	NA	NA	NA
15	46/ M	AG	II	814	II	4 0	CR/ A	619/ 76 0	N	1 2/ 30.9	NA	NA	NA	NA
16	63/ F	AG	II	574	II	21 1	CR/ A	947/ 165 0	N	1 8/ 8 6	NA	NA	NA	NA
17	67/ M	AG	II	1060	II	7 2	PR/ B	907/ 85 6	M	3 7/ 51 1	NA	NA	NA	NA
18	72/ M	AG	II	1720	II	2.6	CR/ A	656/ 38 1	N	1 6/ 60.7	NA	NA	NA	NA
19	66/ M	AG	III	15200	III	13 9	PR/ B	8540/ 56 2	M	13 3/ 96.1	NA	NA	NA	NA
20	80/ M	AG	IV	1220	II	8 3	PR/ B	680/ 55 7	M	4 1/ 49 3	NA	NA	NA	NA
21	39/ F	ID	III	(1090)	NA	NA	PR/ B	767/ (70 4)	M	17 2/ NA	NA	NA	NA	NA
22	45/ F	AG	II	(2740)	NA	NA	PR/ B	1160/ (42 3)	S	2 6/ NA	CR/ A	387/ (14 1)	N	1 8/ NA
23	57/ M	AG	III	(2970)	NA	NA	PR/ B	2070/ (69 6)	S	4 0/ NA	CR/ A	1560/ (52 5)	N	1 8/ NA
24	67/ F	AG	IV	(2590)	NA	NA	PR/ B	1590/ (61 5)	M	6 4/ NA	PD/ B	4030/ (155 6)	M	12 6/ NA
25	79/ F	AG	I	388	I	10.8	NA	NA	NA	NA	CR/ A	318/ 82 0	N	1 7/ 15 9
26	65/ M	ID	II	846	II	6 2	NA	NA	NA	NA	CR/ A	1220/ 144.2	N	0 74/ 11 9
27	71/ F	ID	II	463	II	12 2	NA	NA	NA	NA	CR/ A	453/ 97.8	N	1.1/ 9 0
28	52/ M	ID	IV	581	III	4 7	NA	NA	NA	NA	CR/ A	496/ 85 4	N	2 0/ 43 9
29	41/ M	ID	I	578	I	3 4	NA	NA	NA	NA	CR/ A	433/ 74 9	N	2.4/ 71 1
30	45/ F	AG	II	907	II	16 9	NA	NA	NA	NA	CR/ A	648/ 71 4	N	1 9/ 11 3
31	28/ F	AG	III	6070	III	15 4	NA	NA	NA	NA	CR/ A	395/ 6 5	N	1 7/ 10 7
32	63/ M	AG	III	2720	III	7.9	NA	NA	NA	NA	PR/ B	1330/ 48.9	S	2 6/ 33 1
33	37/ M	AG	IV	7260	IV	6.6	NA	NA	NA	NA	CR/ A	724/ 10 0	N	1.9/ 28 3
34	70/ F	AG	IV	5170	IV	6 3	NA	NA	NA	NA	CR/ A	428/ 8 3	N	2.0/ 31.2
35	74/ M	AG	IV	2190	IV	10.4	NA	NA	NA	NA	CR/ A	866/ 39 5	N	3 3/ 32 0
36	63/ F	AG	II	(1560)	NA	NA	NA	NA	NA	NA	PR/ B	4750/ (304 5)	S	3 1/ NA
37	47/ M	ID	II	(773)	NA	NA	NA	NA	NA	NA	CR/ A	796/ (103 0)	N	1.6/ NA
38	29/ F	AG	III	(2050)	NA	NA	NA	NA	NA	NA	PR/ B	830/ (40 5)	S	2 9/ NA
39	53/ M	AG	IV	(12200)	NA	NA	NA	NA	NA	NA	CR/ A	704/ (5.7)	N	1 3/ NA
40	61/ F	AG	IV	(24300)	NA	NA	NA	NA	NA	NA	PR/ B	2150/ (8 9)	M	10 2/ NA

ID, indolent lymphoma; AG, aggressive lymphoma;, NA, not available; N, no site;, S, single site; M, multiple sites; % sIL-2R or % SUV, percentages of mid- or post-treatment values as compared to pretreatment values

extended to cover the head and lower extremities. This required three to four bed positions with an acquisition time of 10 min each, resulting in a total scanning time of 30 to 40 min. Images were reconstructed with an ordered subset expectation maximization (OS-EM) algorithm (one iteration with 12 ordered subsets).

PET image analysis

FDG-PET images were first interpreted visually in an independent and blinded manner by two nuclear medicine physicians. The observers were allowed to refer to CT or MRI images whenever the clinical data suggested the presence of inflammatory disease. Any obvious foci of FDG uptake that were increased relative to background and not located in the areas of physiologically increased uptake were considered positive for lymphoma. Equivocal FDG uptake on pretreatment images was considered negative, but it was judged to be positive or negative on mid- and post-treatment images after comparison with pretreatment images. The final diagnosis was made by consensus between the two observers, and the FDG-PET imaging findings were then compared with those of the morphological imaging studies.

Semiquantitative image analysis of the dominant lesion was performed by calculating the SUV, which is the decay-corrected tissue activity divided by the injected dose per patient body weight. A circular region of interest (ROI) approximately 1.2 cm in diameter was placed over the area of maximum uptake in the tumor and two adjacent slices. The SUV was calculated by using the mean maximum activity values within the ROIs of these three slices. If the lesion analyzed before treatment had disappeared and other residual tumors remained in the mid- and/or post-treatment period, the SUV was calculated at the residual lesion and corresponding pretreatment lesion. If abnormal uptake had totally disappeared, the SUV was calculated at the same site as the pretreatment site. This analysis was performed only to monitor disease activity, and thus did not affect the results of visual analysis and clinical diagnosis.

The SUVs and serum sIL-2R values were assessed based on the patient's disease status, as described below. The sensitivity, specificity, and accuracy of the SUV and sIL-2R values were calculated regarding the presence of active disease in the mid- and post-treatment periods. Sensitivity was calculated only in the pretreatment period. An SUV of 2.5 was defined as the cutoff value, based on previous reports.[20] The maximum value of the normal range, 530 U/ml, was used as the cutoff for the serum sIL-2R value.

Evaluation of treatment response

The clinical treatment response was determined based on the revised response criteria for malignant lymphoma.[26] In short, CR was defined as disappearance of all evidence of disease. A post-treatment residual mass of any size is permitted as long as it is PET-negative in patients with typically FDG-avid lymphoma (e.g. diffuse large B-cell lymphoma, Hodgkin's lymphoma, follicular lymphoma, and mantle-cell lymphoma). Partial remission (PR) was defined as regression of measurable disease without new sites. At least a 50% decrease in the sum of the product of the diameters of up to six of the largest dominant nodes or nodal masses should be observed. Stable disease (SD) was defined as failure to attain CR/PR or progressive disease (PD). In relapsed disease or PD, any new lesion or an increase by 50% or more of previously involved sites from the nadir PD should be observed.

Patients in CR status were assigned to group Amid or group Apost, and patients in PR, SD, or PD status in the mid- and post-treatment periods were assigned to group Bmid or group Bpost, respectively. This grouping regarding disease activity in the mid- and post-treatment periods and the presence of active disease in the pretreatment period was used as the gold standard in this study.

Statistical analysis

The Mann-Whitney *U*-test was used to compare SUVs or serum sIL-2R values between two different clinical subgroups. The sensitivity, specificity, and accuracy of the SUV and sIL-2R values were compared using the McNemar test. A P value of less than 0.05 was considered statistically significant.

Results

Representative whole-body FDG-PET images in a patient who obtained a CR in the post-treatment period (patient 2) are shown in Fig. 1.

Pretreatment

Thirty-one patients were evaluated by FDG-PET imaging before the start of chemotherapy (Table 1). There were 6 patients with stage I disease, 11 with stage II, 4 with stage III, and 10 with stage IV. The serum sIL-2R values ranged from 159 to 15 500 U/ml (median, 1120 U/ml) in the 31 patients. Five patients had normal values; thus, the sensitivity of the sIL-2R value was 84%. The sIL-2R value was lower in the patients with stage I/II than in the patients with stage III/IV disease (median, 814 vs 2455 U/ml; $P < 0.005$). This marker was also lower in patients with indolent lymphoma than in those with aggressive lymphoma in both stage I/II and III/IV, but the difference was not statistically significant in the latter (median, 497 vs 971 U/ml; $P < 0.05$; and 1330 vs 5170 U/ml; $P = 0.06$, respectively). Four of the 8 patients with indolent lymphoma in stage I/II disease had normal sIL-2R values and 2 others had slightly elevated values (patients 1 and 26). On the other hand, 8 of the 9 patients with aggressive lymphoma in stage I/II exhibited abnormal sIL-2R values, which were greater than

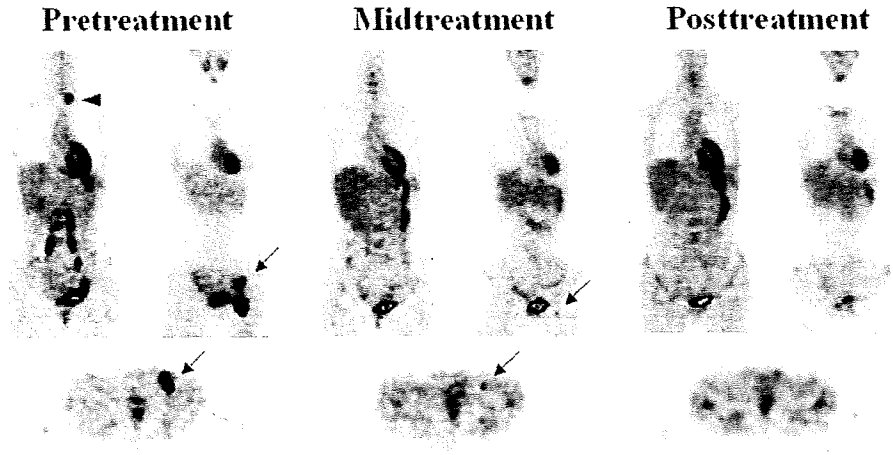

Fig. 1. Whole-body positron emission tomography with a glucose analog, 2-[F-18] fluoro-2-deoxy-D-glucose (FDG-PET) images in a patient with complete remission (CR) in the post-treatment period (patient 2; Table 1). *Pretreatment* period: abnormal uptake was clearly observed in the left supraclavicular (*arrowhead*), bilateral paraaortic/iliac (*white arrowheads*), and left inguinal (*arrow*) sites. Left inguinal uptake was also seen on a transaxial image (*arrow, bottom*). Serum soluble interleukin-2 receptor (sIL-2R) value, 1330 U/ml, and standardized uptake value (SUV), 11.0. *Midtreatment* period: abnormal uptake persisted only in the left inguinal site (*arrows*). (In most of the patients subsequently included in group A in the post-treatment period, no or faint abnormal uptake was observed during this period.) Serum sIL-2R value, 796 U/ml (60%); SUV, 1.9 (17%). *Post-treatment* period: all the abnormal uptake had disappeared. Serum sIL-2R value, 836 U/ml (63% of pretreatment value); SUV, 1.2 (11% of pretreatment value)

1000 U/ml in 4 of the 8 patients. LDH and CRP elevations were observed in only 14 and 10 of all 31 patients, respectively.

Whole-body FDG-PET imaging yielded visually abnormal findings in all 31 patients. Although inability to detect bone marrow involvement resulted in understaging in 4 patients (patients 4, 10, 20, and 28), FDG-PET yielded staging results concordant with morphological imaging studies in all patients. The SUVs at one dominant lesion in each patient ranged from 2.6 to 21.1 (median, 7.7), and all patients would have been thought to have at least one malignant lesion (sensitivity, 100 %; $P = 0.07$ vs sIL-2R sensitivity). There were no differences in the SUVs between the patients with stage I/II and III/IV disease (median, 7.2 vs 7.2, respectively). Nor were any differences observed in the SUVs between the patients with indolent and aggressive lymphoma in either the stage I/II or stage III/IV disease groups (median, 6.1 vs 11.2, and 6.7 vs 8.3, respectively), although the values tended to be higher in the latter. Even in the 5 patients exhibiting normal sIL-2R values (patients 6, 8, 14, 25, and 27), FDG-PET imaging yielded abnormal findings visually, with SUVs of more than 2.5.

Assessment of the treatment outcome in the 31 patients who had pretreatment PET examinations showed a CR in 25 patients at the end of treatment. There was no relationship between treatment outcome and the serum sIL-2R values or FDG-PET findings obtained in this period.

Midtreatment

Twenty-four patients were examined by FDG-PET after three or four cycles of chemotherapy. Twenty of them had undergone pretreatment PET studies. Eight patients were evaluated as having a CR and 16 as having PR, based on the morphological imaging studies. The 8 CR and 16 PR patients were assigned to groups Amid and Bmid, respectively, and their disease activity proved to be correct based on the follow-up results. The data for each patient are listed in Table 1.

The serum sIL-2R values ranged from 105 to 1830 U/ml in the 8 group Amid patients, and from 436 to 8540 U/ml in the 16 group Bmid patients. Only 2 of the 8 group Amid patients had normal values, as opposed to 15 of the 16 group Bmid patients exhibiting abnormal values. The sensitivity, specificity, and accuracy of the sIL-2R value were 94%, 25%, and 71%, respectively. The 2 group Amid patient (patients 8 and 14) and 1 group Bmid patient (patient 6) with normal values had exhibited normal sIL-2R values in the pretreatment period as well. Inflammation/infection must have been responsible for the elevated values in this period in 2 of the remaining 6 group Amid patients (patients 9 and 16);[5–7] however, the reasons for the elevated values in the other 4 patients were unclear. Five of the 6 group Amid patients with elevated values had elevated values again in the post-treatment period. There was no significant difference between the sIL-2R values in group Amid and group Bmid patients (median, 638 vs 839 U/ml, respectively).

FDG-PET allowed visual and semiquantitative evaluation of disease activity and changes in response to treatment in all the patients. The SUVs ranged from 0.84 to 2.8 in the 8 group Amid patients, and from 1.5 to 17.2 in the 16 group Bmid patients. Five group Bmid patients exhibited SUVs of less than 2.5, although visual PET findings were all positive. The sensitivity, specificity, and accuracy of the SUV were 69%, 88%, and 75%, respectively. No statistically significant differences were observed between the SUV and

sIL-2R in any of the parameters above, with the specificity for SUV and sIL-2R being 25% and 88%, respectively. The SUV was significantly lower in the group Amid than in the group Bmid patients (median, 1.7 vs 3.2; $P < 0.005$, respectively).

Of 20 patients who underwent pretreatment PET studies (all responders), 19 exhibited decreased serum sIL-2R values in this period (range, 8%-95% of the pretreatment values). Patient 16, in CR status, had an elevated sIL-2R value that was higher than the pretreatment value because of pneumonia. All 20 patients also exhibited decreased SUVs (range, 8.6%-96.1% of the pretreatment values).

The 24 patients who had PET examinations in this period included 7 patients assigned to group B at the end of treatment, 4 as PR and 3 as PD. The serum sIL-2R value in this period did not differ between the patients in group A and B later, in the post-treatment period (group Apost and Bpost; median, 796 vs 862 U/ml, respectively). On the other hand, the SUV in this period was significantly lower in the patients later included in group Apost than in those included in group Bpost (median, 1.9 vs 4.1; $P < 0.001$, respectively). The same was true even when the data were restricted to the 16 patients in group Bmid in this period (excluding 8 group Amid patients from all 24 patients). The serum sIL-2R value in this period did not differ between the patients in groups A and B later in the post-treatment period (median, 816 vs 862 U/ml, respectively; Fig. 2), while the SUV was significantly lower in the patients in group Apost than in the patients in group Bpost (median, 2.3 vs. 4.1; $P < 0.005$, respectively; Fig. 2).

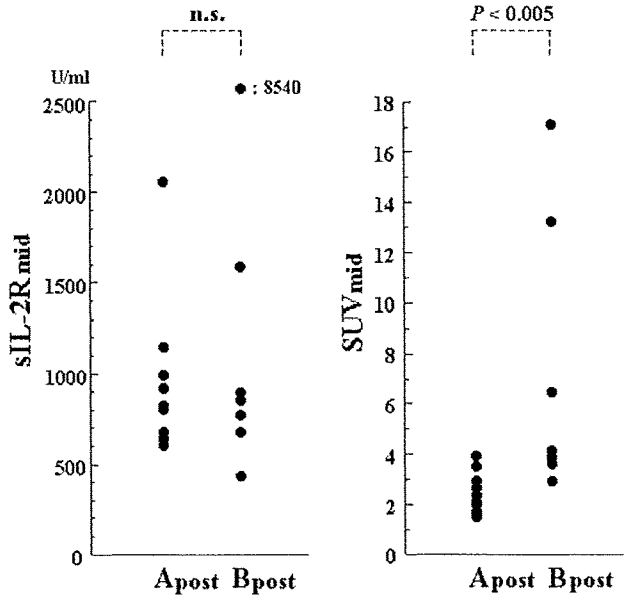

Fig. 2. Relationship between serum sIL-2R value (*left*) or SUV (*right*) in group Bmid and the post-treatment grouping. (Note re groups: patients in CR status were assigned to group Amid or group Apost, and patients in partial remission (PR), stable disease (SD), or progressive disease (PD) status in the mid- and post-treatment periods were assigned to group Bmid or group Bpost, respectively.) The sIL-2R value in group Bmid did not differ between the patients in groups Apost and Bpost (median sIL-2R value, 816 U/ml in group Apost and 862 U/ml in group Bpost). The SUV in the patients in group Bmid was significantly lower in the patients in group Apost than group Bpost (median SUV, 2.3 in group Apost and 4.1 in group Bpost; $P < 0.005$). *Apost*, Group Apost; *Bpost*, group Bpost; *n.s.*, not significant; *mid*, midtreatment

Post-treatment

Twenty-four patients were examined by FDG-PET after the completion of chemotherapy. Sixteen of them had undergone pretreatment PET studies and 8 of them had undergone midtreatment PET studies. Nineteen patients were evaluated as CR (group Apost), 4 as PR, and 1 as PD (group Bpost), and their disease activity proved to be correct based on the follow-up results. The data for each patient are listed in Table 1. Three patients having radiation therapy were evaluated in this period. However, none of the patients showed abnormal FDG uptake at the radiation sites.

The serum sIL-2R values ranged from 318 to 1560 U/ml and from 830 to 4750 U/ml, respectively, in the 19 group Apost patients and 5 group Bpost patients. Nine of the 19 group Apost patients exhibited normal values, whereas all 5 group Bpost patients exhibited abnormal values. Thus the sensitivity, specificity, and accuracy of the sIL-2R value were 100%, 47%, and 58%, respectively. Inflammation/infection must have been the reason for the elevated values in 4 of the 10 group Apost patients (patients 5, 23, 33, and 35), but no clear explanation was found in the other 6 patients in group Apost. Two group Apost patients with normal values (patients 25 and 27) had exhibited normal values in the pretreatment period as well. The serum sIL-2R was significantly lower in the group Apost patients than in the group Bpost patients (median, 648 vs 2150 U/ml; $P < 0.005$, respectively).

FDG-PET imaging exhibited findings concordant with the morphological imaging in 22 of the 24 patients. The remaining 2 patients (patient 37 [Fig. 3] and patient 39) had residual masses without positive FDG uptake, and they proved to represent inactive disease according to the subsequent follow-up results (group Apost). The SUVs ranged from 0.74 to 3.3 and from 2.6 to 12.6, respectively, in the 19 group Apost and in the 5 group Bpost patients. There was only a little overlap in the SUVs, due to patient 35, between the two patient groups. The SUV was significantly lower in the group Apost than in the group Bpost patients (median, 1.7 vs 3.1, respectively; $P < 0.005$). The sensitivity, specificity, and accuracy of the SUV were 100%, 95%, and 96%, respectively (specificity and accuracy, $P < 0.01$ vs sIL-2R). Patient 23 had a high sIL-2R value and was suspected of having an intravenous hyperalimentation (IVH)-related infection, and this was clearly demonstrated by FDG-PET.

Of 16 patients who had undergone pretreatment PET studies (all responders), 13 and 14 exhibited decreased serum sIL-2R values (7%–98% of pretreatment values) and decreased SUVs (8%–77% of pretreatment values), respectively, in this period. Seven of the 8 patients who had undergone midtreatment PET examinations were considered to

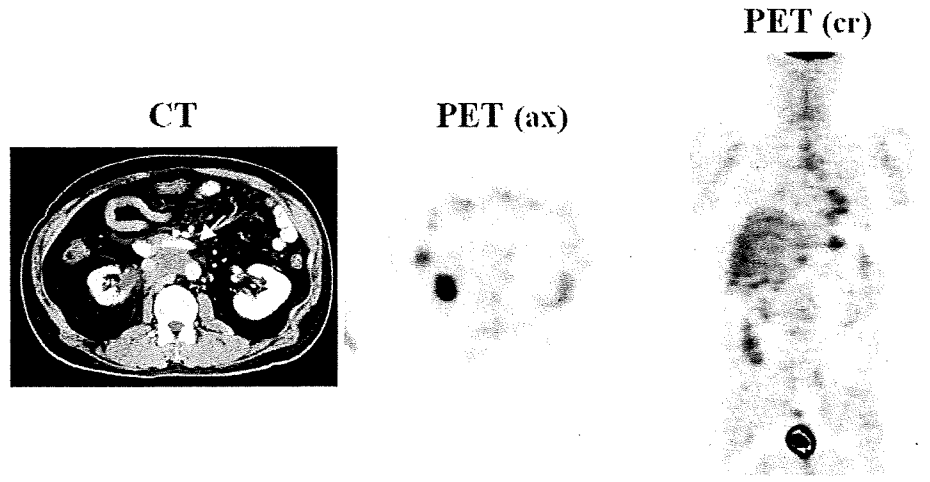

Fig. 3. Paraaortic mass without positive FDG uptake in the post-treatment period (patient 37). Computed tomography (CT): a soft-tissue-density mass was depicted in the paraaortic site (*white arrow*). PET: neither the transaxial (*ax*) nor the coronal FDG-PET (*cr*) images showed positive uptake at the corresponding site. Follow-up CT revealed a mass the same size as that on the original CT, indicating no, or almost no activity in it. Serum sIL-2R value, 796 U/ml; SUV, 1.6

be responders in this period. Of them, 5 and 7 exhibited decreased sIL-2R values (33%–80% of midtreatment value) and decreased SUVs (29%–81% of midtreatment value), respectively. Patients 2 and 3 showed higher sIL-2R values than those seen in the midtreatment period; however, the reasons for the elevations were unclear. Figure 4 shows whole-body FDG-PET images in a patient with PD (patient 24) in this period; it is noteworthy that intense abnormal uptake was observed in the thoracic spine in the midtreatment period.

Discussion

In our study, before the start of chemotherapy the serum sIL-2R value was lower in the patients with stage I/II than in those with stage III/IV disease, and it tended to be lower in patients with indolent than in those with aggressive lymphoma within the same stage groups. These results were as expected according to the published data[8,10,12–14] and were considered to reflect the total disease activity in each patient. However, the small elevations of the sIL-2R values in the pretreatment period in low-stage or low-grade NHL may be problematic when using the serum sIL-2R value as a tumor marker in clinical situations. Among the 31 patients evaluated before treatment in this study, there were 5 patients with normal sIL-2R values (sensitivity, 84 %) and 4 with only slightly elevated values (less than 700 U/ml). As neither the LDH nor CRP values were elevated in these 9 patients, evaluation with hematological markers after treatment or follow-up tended to be difficult.

Whole-body FDG-PET imaging, on the other hand, yielded abnormal findings in all patients before treatment in our study. Disease extension and the activity of each lesion depicted by this imaging method enabled better understanding of disease status in all patients. The SUVs at the dominant lesions were greater than 2.5 (the value reported as the cutoff for malignancy in previous studies[20]) in all patients, including the 5 with normal sIL-2R values (sensitivity, 100%). These results demonstrated that whole-body FDG-PET imaging allowed accurate evaluation of NHL activity as a baseline in the pretreatment period, more so than the serum sIL-2R values did.

Of the 40 patients involved in the present study, 30 were included in group A in the post-treatment period (including 11 without PET examinations), but only 13 of these 30 patients exhibited normal serum sIL-2R values at that time. Although 4 additional patients exhibited normal values in the subsequent follow-up period, a substantial overlap of serum sIL-2R values was observed between the patients in the pretreatment period and patients in group Apost, especially in those with low-stage or low-grade disease. This finding, which has already been reported,[10,14] seems to indicate the unreliability of this marker after treatment as well. Although, in most of responding patients, the sIL-2R value post-treatment was lower than that before treatment, the sIL-2R occasionally exhibited higher abnormal values than in the pretreatment period. Infection/inflammation was considered to be the reason for the elevated sIL-2R values clinically, as this is known to cause elevation of the values.[5–7] Other possible reasons for the elevation include aging,[6] smoking habit,[10] or subtle treatment-related inflammatory processes. In any event, abnormal serum sIL-2R values for reasons other than NHL activity cause confusion in clinical situations.

Whole-body FDG-PET imaging provided accurate information on the disease status of each patient in our study in both the mid- and post-treatment periods. The SUVs allowed more accurate evaluation of disease activity than the serum sIL-2R values. The specificity and accuracy of the SUV were significantly higher than those of the sIL-2R value in the post-treatment period (95% vs 47% and 96% vs 58 %, respectively), and the specificity of the SUV tended to be higher than that of the sIL-2R value in the midtreatment period (88% vs 25%). The SUV was significantly lower in the group A than in the group B patients in the midtreatment period, whereas the sIL-2R was not different.

Several group B patients had relatively low SUVs in the midtreatment period despite having gross residual active disease. Of note is that the status in all of them was changed

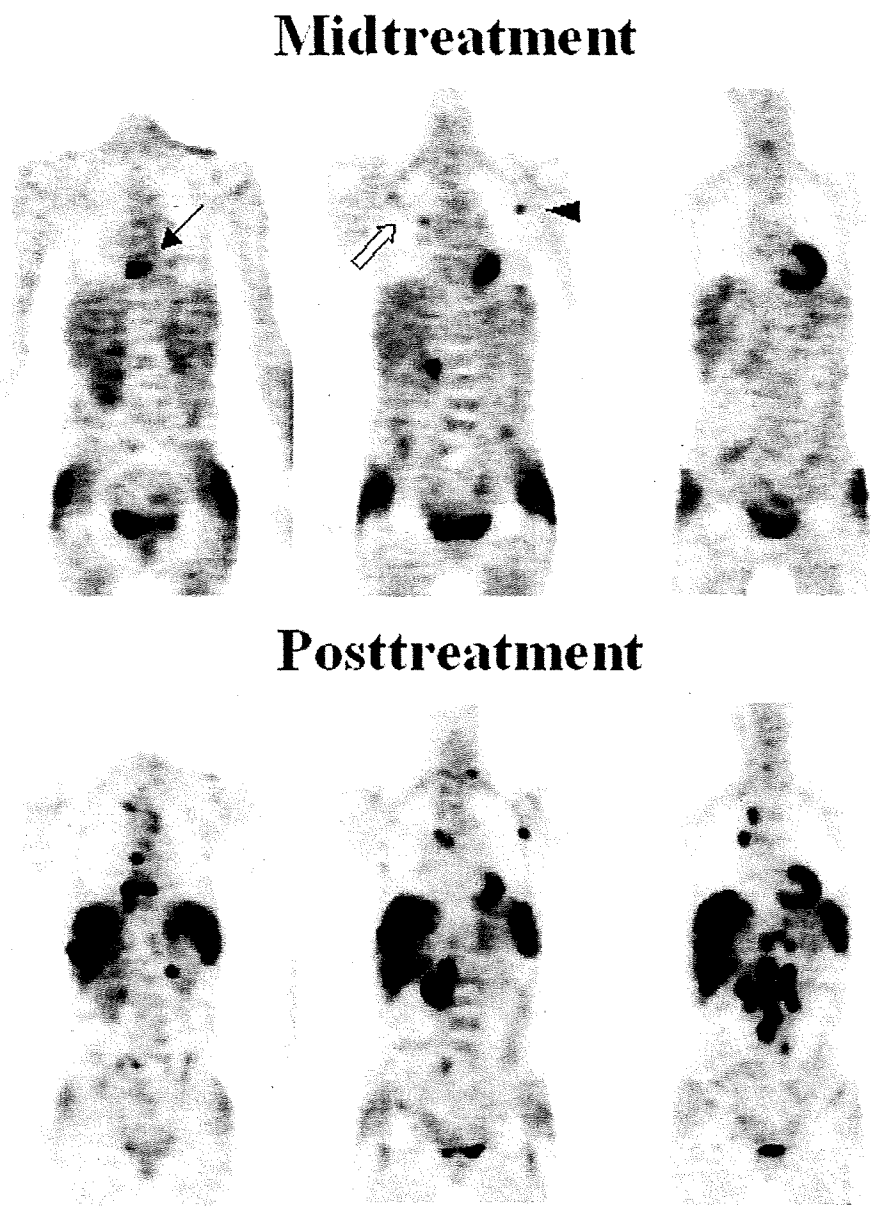

Fig. 4. Whole-body FDG-PET images in a patient exhibiting PD in the post-treatment period (patient 24). *Midtreatment* period: intense abnormal uptake persisted in the thoracic spine (*arrow, left*) in addition to the intermediate uptake in the left axillary site (*arrowhead*). (Patients with persistent intense uptake in this period tended to be included in group B later in the post-treatment period.) Serum sIL-2R value, 1590 U/ml; SUV, 6.4. *Open arrow*, Post-inflammatory change. *Post-treatment* period: abnormal uptake was observed in multiple sites, including the liver, spleen, and paraaortic site. Serum sIL-2R value, 4030 U/ml; SUV, 12.6

to group A in the post-treatment period, along with the patients whose group A status had been continued since the midtreatment period. By contrast, the status of group Bmid patients with high SUVs tended not to change to that of group Apost patients. In this respect, Wahl et al.[23] demonstrated data in their study of breast cancer patients suggesting that effective chemo- or chemohormonotherapy caused a rapid and significant decrease in tumor metabolic activity, within days, that preceded a decrease in tumor size. Our findings are consistent with theirs, although tumor FDG uptake was not measured serially in our study.

There are certain limitations in the present study. First, most of the patients underwent only either a mid- or post-treatment FDG-PET study. Thus, we did not evaluate the changes in SUVs and sIL-2R values between pre- and mid- or post-treatment status. Poor physical condition, due to the side effects of chemotherapy, or a crowded PET machine schedule, prevented patients from receiving midtreatment PET examinations. Patients with a CR and no abnormal FDG uptake in the midtreatment period did not undergo post-treatment PET studies, because their post-treatment status was regarded as being the same as the midtreatment status, based on the clinical evaluation at the time. Second, the results of the clinical evaluations and FDG-PET studies were not confirmed histopathologically in most of the lesions, especially after treatment. For ethical reasons, close follow up was the only method used to confirm the results: this is an inevitable problem inherent in lymphoma research in general. Another limitation may be that most of the patients in our study had only one residual disease site after

treatment. The usefulness of whole-body FDG-PET imaging in the mid- or post-treatment period may therefore not be fully validated. Although post-treatment PET studies were performed more than 10 days after completion of chemotherapy in this study, the timing was earlier than that recommended by the revised response criteria for malignant lymphoma.[26] Our timing was decided considering the clinical situations and was based on some published reports in which lymphoma lesions were evaluated with PET 7–10 days after chemotherapy.[20,27] The frequency of false-positive findings was low in our study.

In conclusion, comparison with the serum sIL-2R marker showed that the SUV of FDG-PET imaging tended to be more sensitive in patients with stage I/II or indolent NHL before treatment, and the SUV was more specific for evaluating disease activity in patients with a CR status after treatment intervention. The SUV was considered to be a useful tumor marker for NHL activity before, during, and after chemotherapy.

References

1. Peterson BA (1999) Current treatment of follicular low-grade lymphomas. Semin Oncol 26:2–11
2. Coiffier B (1999) Treatment of aggressive non-Hodgkin's lymphoma. Semin Oncol 26:12–20
3. Hauke RJ, Armitage JO (2000) Treatment of non-Hodgkin lymphoma. Curr Opin Oncol 12:412–418
4. Kaminski MS, Estes J, Zasadny KR, et al. (2000) Radioimmunotherapy with iodine (131) I tositumomab for relapsed or refractory B-cell non-Hodgkin lymphoma: updated results and long-term follow-up of the University of Michigan experience. Blood 96:1259–1266
5. Pizzolo G, Chilosi M, Semenzato G (1987) The soluble interleukin-2 receptor in haematological disorders. Br J Haematol 67:377–380
6. Rubin LA, Nelson DL (1990) The soluble interleukin-2 receptor: biology, function, and clinical application. Ann Intern Med 113: 619–627
7. Zerler B (1991) The soluble interleukin-2 receptor as a marker for human neoplasia and immune status. Cancer Cells 3:471–479
8. Chilosi M, Semenzato G, Vinante F, et al. (1989) Increased levels of soluble interleukin-2 receptor in non-Hodgkin's lymphomas. Relationship with clinical, histologic, and phenotypic features. Am J Clin Pathol 92:186–191
9. Barak V, Ginzburg M, Kalickman I, et al. (1992) Serum soluble interleukin-2 receptor levels are associated with clinical disease status and histopathological grade in non-Hodgkin's lymphoma and chronic lymphocytic leukemia. Leuk Lymphoma 7:431–438
10. Motokura T, Kobayashi Y, Fujita A, et al. (1995) Clinical significance of serial measurement of the serum levels of soluble interleukin-2 receptor and soluble CD8 in malignant lymphoma. Leuk Lymphoma 16:355–362
11. Wagner DK, Kiwanuka J, Edwards BK, et al. (1987) Soluble interleukin-2 receptor levels in patients with undifferentiated and lymphoblastic lymphomas: correlation with survival. J Clin Oncol 5:1262–1274
12. Pui CH, Ip SH, Kung P, et al. (1987) High serum interleukin-2 receptor levels are related to advanced disease and a poor outcome in childhood non-Hodgkin's lymphoma. Blood 70:624–628
13. Stasi R, Zinzani L, Galieni P, et al. (1994) Detection of soluble interleukin-2 receptor and interleukin-10 in the serum of patients with aggressive non-Hodgkin's lymphoma. Identification of a subset at high risk of treatment failure. Cancer 74:1792–1800
14. Kono N, Kanda Y, Yamamoto R, et al. (2000) Prognostic significance of serum soluble interleukin-2 receptor level in non-Hodgkin's lymphoma: a single center study in Japan. Leuk Lymphoma 37:151–156
15. Delbeke D (1999) Oncological applications of FDG PET imaging: brain tumors, colorectal cancer, lymphoma and melanoma. J Nucl Med 40:591–603
16. Delbeke D (1999) Oncological applications of FDG PET imaging. J Nucl Med 40:1706–1715
17 Gambhir SS, Czernin J, Schwimmer J, et al. (2001) A tabulated summary of the FDG PET literature. J Nucl Med 42:1S–93S
18. Hoh CK, Glaspy J, Rosen P, et al. (1997) Whole-body FDG-PET imaging for staging of Hodgkin's disease and lymphoma. J Nucl Med 38:343–348
19. Moog F, Bangerter M, Diederichs CG, et al. (1997) Lymphoma: role of whole-body 2-deoxy-2-[F-18] fluoro-D-glucose (FDG) PET in nodal staging. Radiology 203:795–800
20. Romer W, Hanauske AR, Ziegler S, et al. (1998) Positron emission tomography in non-Hodgkin's lymphoma: assessment of chemotherapy with fluorodeoxyglucose. Blood 91:4464–4471
21. Jerusalem G, Beguin Y, Fassotte MF, et al. (1999) Whole-body positron emission tomography using 18F-fluorodeoxyglucose for post-treatment evaluation in Hodgkin's disease and non-Hodgkin's lymphoma has higher diagnostic and prognostic value than classical computed tomography scan imaging. Blood 94:429–433
22. Weber WA, Schwaiger M, Avril N (2000) Quantitative assessment of tumor metabolism using FDG-PET imaging. Nucl Med Biol 27:683–687
23. Wahl RL, Zasadny K, Helvie M, et al. (1993) Metabolic monitoring of breast cancer chemohormonotherapy using positron emission tomography: initial evaluation. J Clin Oncol 11:2101–2111
24. Harris NL, Jaffe ES, Diebold J, et al. (2000) Lymphoma classification – from controversy to consensus: The R.E.A.L. and WHO Classification of lymphoid neoplasms. Ann Oncol 11 (Suppl 1):3–10
25. Harris NL, Jaffe ES, Diebold J, et al. (1999) World Health Organization classification of neoplastic diseases of the hematopoietic and lymphoid tissues: report of the Clinical Advisory Committee meeting, Airlie House, Virginia, November 1997. J Clin Oncol 17:3835–3849
26. Cheson BD, Pfistner B, Juweid ME, et al. (2007) Revised response criteria for malignant lymphoma. J Clin Oncol 25:579–586
27 Mikhaeel NG, Timothy AR, Hain SF, et al. (2000) 18-FDG-PET for the assessment of residual masses on CT following treatment of lymphomas. Ann Oncol 11 (Suppl 1):147–150

Intravascular Lymphomatosis Initially Suspected from Uterine Cytology

A Case Report

Itsuko Nakamichi, M.D., Kouki Shimazu, M.D., Jun-ichiro Ikeda, M.D., Amane Yamauchi, M.D., Ph.D., Jun Ishiko, M.D., Ph.D., Masao Mizuki, M.D., Ph.D., Yuzuru Kanakura, M.D., Ph.D., and Katsuyuki Aozasa, M.D., Ph.D.

Background

Because recognizable lesions are often absent, selection of biopsy sites for diagnosis of intravascular large B-cell lymphoma (IVL) is frequently problematic.

Case

A 59-year-old woman was admitted with fever and general fatigue. Combined physical and roentgenographic examinations revealed neither lymphadenopathy, hepatosplenomegaly nor mass lesions in other organs. Serum lactate dehydrogenase level was 1,412 IU/L. There were no genital symptoms, but uterine cytologic examination revealed large cells distributed in a noncohesive pattern. These cells had a large, irregularly shaped nucleus in which several nucleoli were discernible and showed positive immunoreactivity for leukocyte common antigen. Three months after admission, neurologic symptoms appeared, and magnetic resonance imaging revealed multiple nodular lesions in the brain. Biopsy specimens from the brain lesion showed the proliferation of large lymphoid cells filling the lumina of small vessels and Virchow-Robin's space. Immunohistochemistry revealed that the tumor cells were positive for CD20 and CD79a but negative for CD3, indicative of IVL.

Conclusion

Uterine cytologic and/or histologic examinations could be the choice for diagnosis of IVL, even when genital symptoms are absent. (Acta Cytol 2009;53:198–200)

Keywords: intravascular lymphomatosis, lymphoma, Papanicolaou smear.

Not only cytologic examination but also histologic evaluation of the uterine cavity with the aid of immunohistochemistry is much less invasive than brain biopsy and might provide a clue to the diagnosis of IVL.

Intravascular large B-cell lymphoma (IVL), a variant of diffuse large B-cell lymphoma, is a rare disease, comprising 0.17% (4 of 2,303) of all malignant lymphoma registered in the Osaka Lymphoma Study Group, Japan, and 0.4% in the literature from western countries.[1] Tumor cells are exclusively found in the lumina of small vessels and lack a tendency for mass formation, at least at the early stage of the disease. Clinical symptoms are caused by occlusion of small vessels by tumor cells; they include skin lesions and neurologic symptoms.[2] Because recognizable lesions are absent or, if present, not specific, selection of biopsy sites for diagnosis of IVL is frequently problematic. Below we present a case of IVL in which tumor cells were detected at uterine cytologic examination.

Case Report

A 59-year-old woman was admitted to Osaka University Hospital with fever and general fatigue. Ten years before the admission, she had been shown to have a high level of serum lactate dehydrogenase (LDH), with values ranging from 543 to 871 IU/L. Combined physical and roentgenographic examinations did not reveal either lymphadenopathy, hepatosplenomegaly or other mass lesions except for a small, leiomyomatous nodule in the uterus. Laboratory data showed serum values of LDH 1,412 IU/L, aspartate aminotransferase 133 IU/L, alanine aminotransferase 55 IU/L, γ-glutamyl transpeptidase 85 U/L, alkaline phosphatase 529 U/L, soluble IL-2-R 1870 IU/mL, neuron-specific enolase 42.3 ng/mL and ferritin 174 ng/mL. Peripheral blood cells were normal in count and morphology. Bone marrow puncture revealed no abnormal cells.

Uterine cytologic examination suggested the presence of malignant hematopoietic cells. Then endometrial curettage was performed, revealing infiltration of normal-looking inflammatory cells with no evident lymphoma cells. Three months after the admission,

From the Departments of Pathology and of Hematology and Oncology, Osaka University Graduate School of Medicine, Osaka, Japan.

Drs. Nakamichi, Shimazu, Ikeda and Yamauchi are Associate Professors, Department of Pathology.

Drs. Ishiko and Mizuki are Associate Professors, Department of Hematology and Oncology.

Dr. Kanakura is Professor, Department of Hematology and Oncology.

Dr. Aozasa is Professor, Department of Pathology.

Supported in part by grant 16390105 from the Ministry of Science, Culture and Sports, Japan.

Address correspondence to: Amane Yamauchi M.D., Ph.D., Department of Pathology (C3), Osaka University Graduate School of Medicine, 2-2 Yamadaoka Suita, Osaka 565-0871, Japan (yamauchi@molpath.med.osaka-u.ac.jp).

Financial Disclosure: The authors have no connection to any companies or products mentioned in this article.

Received for publication June 13, 2007.

Accepted for publication August 8, 2007.

 0001-5547/09/5302-0198/$21.00/0

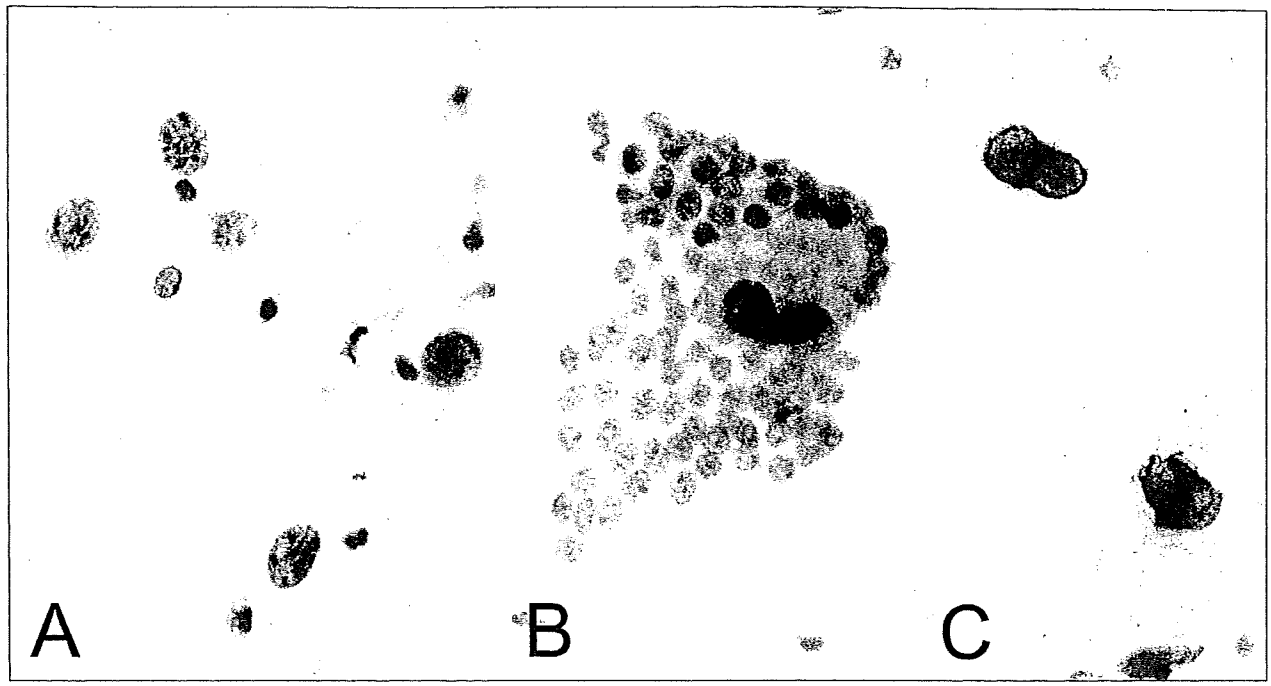

Figure 1 (A and B) Noncohesive, large cells with high nuclear/cytoplasmic ratio together with clusters of normal endometrial epithelial cells. The large cells had a large, oval nucleus with thin nuclear membrane with multiple distinct nucleoli (Papanicolaou stain, ×400). (C) The large cells were positive for leukocyte common antigen (avidin-biotin complex method, ×400).

mild splenomegaly appeared. Then laparoscopic splenectomy and wedge biopsy of the liver were performed for a definitive diagnosis of lymphoma. The weight of the spleen was 335 g. Histologically obvious tumorous lesions could not be identified in the spleen. Immunohistochemistry revealed a few large lymphoid cells with CD20+, but a diagnosis of B-cell lymphoma was not possible because of the quite small number of these cells in the red pulp. In the liver, no abnormal cells were found. Neurologic symptoms, such as disturbance of memory and scintillating scotoma, appeared. Magnetic resonance imaging revealed multiple lesions in the brain; then a stereostatic brain biopsy was performed. Histologic diagnosis was IVL.

Chemotherapy with rituximab, vincristine, cyclophosphamide, prednisolone and doxorubicin was started, and the neurologic symptoms disappeared soon. Clinical findings with the main emphasis on the movement of LDH levels in this case were reported elsewhere.[3]

Pathologic Findings

Cytologic Findings. Because of the presence of a small nodule, possibly leiomyoma, in the uterus, cytologic examination was performed, revealing the presence of noncohesive, large cells with high nuclear/cytoplasmic ratio together with clusters of normal endometrial epithelial cells (Figure 1). These cells had a large, oval nucleus with thin nuclear membrane in which distinct nucleoli were discernible. Large cells with folded or multilobated nucleus were occasional. These cells were positive for leukocyte common antigen, suggesting malignant hematopoietic cells. A cytologic diagnosis of possible malignant lymphoma was made.

Histologic Findings. Biopsy specimens from the brain showed that lumina of the small vessels and Virchow-Robin space were filled with large lymphoid cells. These cells were positive for CD20 and CD79a but negative for CD3, confirming the diagnosis of IVL (Figure 2).

Discussion

IVL is a rare disease and affects elderly patients (median age, 70 years; range, 34–90; male:female ratio 0.9).[4] The disease is hard to diagnose accurately because of the absence of mass lesions and appearance of nonspecific clinical symptoms, including skin eruption and neurologic disturbance.[4,5] They are the main reasons for delay in diagnosis, thus resulting in a delay in employment of effective chemotherapy. As a result, IVL usually run an aggressive course. The median survival is 12 months, and 3-year survival is 14–32%.[4,6] Approximately 50–60% of cases of IVL show remission in response to chemotherapy.[4] Therefore, early diagnosis of the disease is essential for improving the prognosis of IVL.

The present patient did not show gynecologically abnormal findings, such as abnormal genital bleeding, but uterine cytologic examination was done by chance because of a roentgenographically detected leiomyomatous nodule. In the cytologic smears, there were large cells distributed in a noncohesive manner. These cells had morphologies identical to those of germinal center cells: large cells with an oval nucleus (centroblasts) or folded nucleus (cleaved). Immunohistochemistry with CD45 on the uterine cytologic smears suggested characteristics of hematologic cells and, with a battery of antibodies on the histologic samples from the brain, confirmed the diagnosis of IVL.

A previous study showed the intravascular proliferation of tumor cells of IVL in systemic organs, such as brain, skin, bone marrow, liver, spleen, lung and kidney, with no tendency for tumor formation.[7] Therefore, it is difficult to select organs for biopsy without signs and symptoms indicating involvement of specific organs by IVL. Under such conditions, the brain and skin are main targets for biopsy, but the brain biopsy is quite invasive and not easily under-

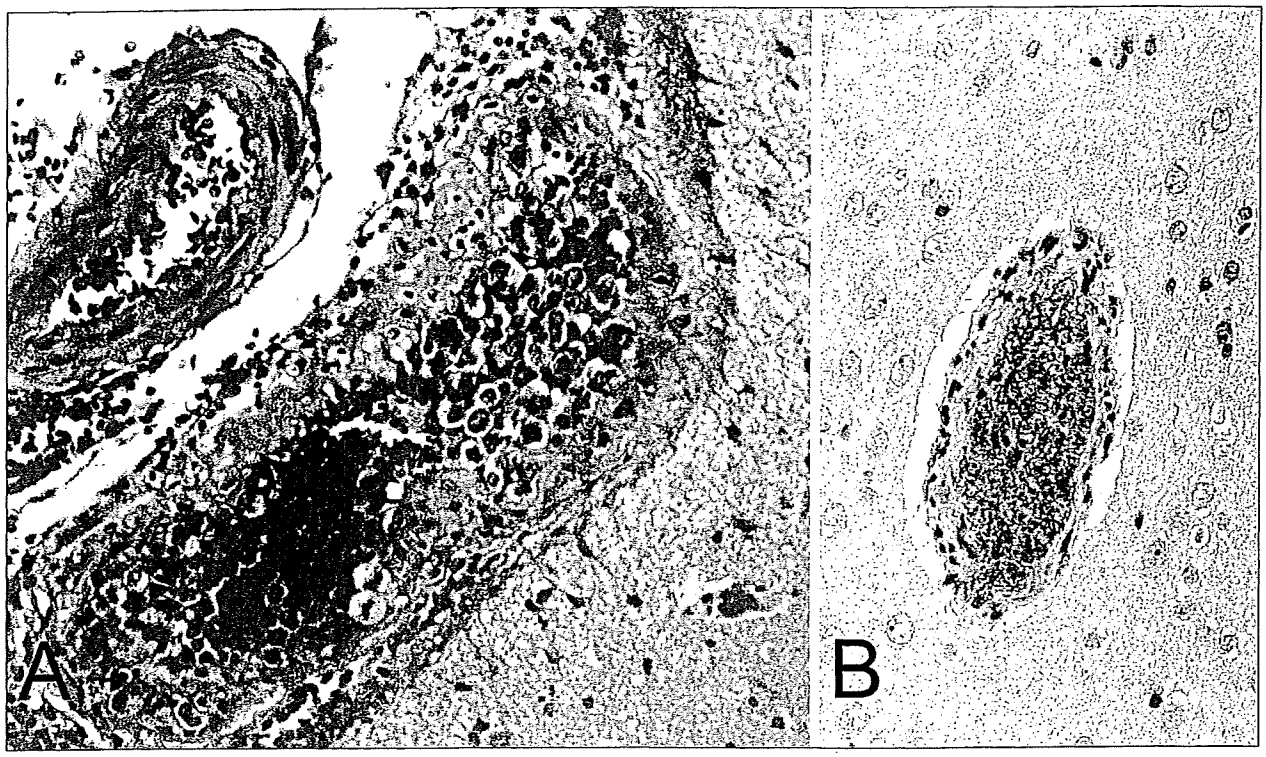

Figure 2 (A) Biopsy specimens from the brain showed that lumina of the small vessels were filled with large lymphoid cells (hematoxylin-eosin, ×400). (B) These cells were positive for CD20 (avidin-biotin complex method, ×400).

taken. In this respect, the uterine endometrium could be another target for morphologic diagnosis of IVL. Not only cytologic examination but also histologic evaluation of the uterine cavity with the aid of immunohistochemistry is much less invasive than brain biopsy and might provide a clue to the diagnosis of IVL.

References

1. Bouzani M, Karmiris T, Rontogianni D, Delimpassi S, Apostolidis J, Mpakiri M, Nikiforakis E: Disseminated intravascular B-cell lymphoma: Clinicopathological features and outcome of three cases treated with anthracycline-based immunochemotherapy. Oncologist 2006;11:923–928
2. Gatter KC, Warnke RA: Intravascular large B-cell lymphoma. *In* World Health Organization Classification of Tumours: Pathology and Genetics of Tumours of Haematopoietic and Lymphoid Tissues. Edited by ES Jaffe, NL Harris, H Stein, JW Vardiman. Lyon, IARC Press, 2001, pp 177–178
3. Ishiko J Mizuki M, Yasumi M, Ujiie H, Nakamichi I, Yoshino K, Hoshimoto N, Izumoto S, Hiramatsu N, Aozasa K, Kanakura Y: An indolent subtype of 'intravascular lymphoma': A case with a three year history of LDH elevation. Leuk Lymph 2007:48:1872–1874
4. Ferreri AJ, Campo E, Seymour JF, Willemze R, Ilariucci F, Ambrosetti A, Zucca E, Rossi G, López-Guillermo A, Pavlovsky MA, Geerts ML, Candoni A, Lestani M, Asioli S, Milani M, Piris MA, Pileri S, Facchetti F, Cavalli F, Ponzoni M: Intravascular lymphoma: Clinical presentation, natural history, management and prognostic factors in a series of 38 cases, with special emphasis on the 'cutaneous variant.' Br J Haematol 2004;127:173–183
5. Zuckerman D, Seliem R, Hochberg E: Intravascular lymphoma: The oncologist's "great imitator." Oncologist 2006;11:496–502
6. DiGiuseppe JA, Nelson WG, Seifter EJ, Boitnott JK, Mann RB: Intravascular lymphomatosis: A clinicopathologic study of 10 cases and assessment of response to chemotherapy. J Clin Oncol 1994;12:2573–2579
7. Bogomolski-Yahalom V, Lossis IS, Okun E, Sherman Y, Lossos A, Polliack A: Intravascular lymphomatosis: An indolent or aggressive entity. Leuk Lymphoma 1998;29:585–593